

FIG. 1. Effective energy of ground level  $J = \frac{1}{2}$  in the presence of a radiofrequency field.

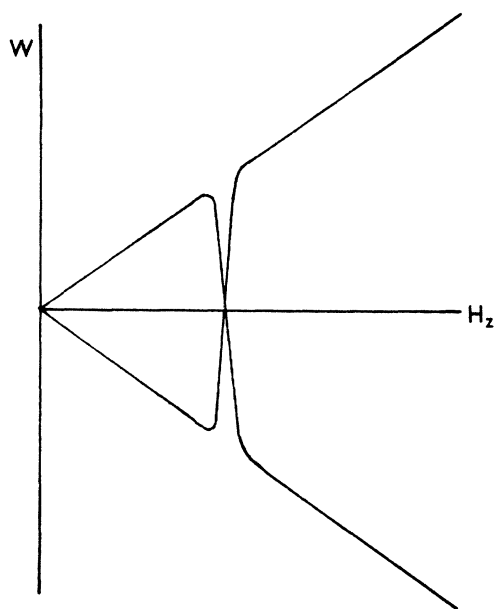


FIG. 2. Mean energy according to Bitter.

quencies are those which are associated with the non-vanishing matrix elements of electric dipole moment coupling ground and excited states, which are simply calculated from the time-dependent wave functions quoted by Bitter. These frequencies are such as would occur if the ground level had energies

$$E = \pm \frac{1}{2} \hbar \omega \pm \frac{1}{2} [\hbar^2 (\omega_0 - \omega)^2 + (g\mu_0 H_0)^2]^{\frac{1}{2}}. \quad (1)$$

In this expression all four combinations of the  $\pm$  signs are to be taken. The appearance of four effective energy values, instead of two, can be understood in terms of the possibility of the emission or absorption of one quantum or no quantum by the radiofrequency field. The intensities of the lines are obtained from the intensities in the absence of radiofrequency field, by multiplying

by a factor

$$\frac{1}{2} \left[ 1 \pm \frac{\hbar(\omega_0 - \omega)}{[\hbar^2(\omega_0 - \omega)^2 + (g\mu_0 H_0)^2]^{\frac{1}{2}}} \right], \quad (2)$$

the sign being + if the two signs are equal in Eq. (1) and - if unequal.

Equation (1) for the effective energy should be contrasted with Bitter's result for the mean energy,

$$\begin{aligned} W &= \pm \frac{1}{2} g\mu_0 H_z \left[ \frac{\delta + H_0/H_z}{(1 + \delta^2)^{\frac{1}{2}}} \right] \\ &\equiv \pm \frac{1}{2} \hbar \omega_0 \left[ \frac{\hbar(\omega - \omega_0) + g\mu_0 H_0^2/H_z}{[\hbar^2(\omega_0 - \omega)^2 + (g\mu_0 H_0)^2]^{\frac{1}{2}}} \right]. \end{aligned} \quad (3)$$

The two expressions are plotted in Figs. 1 and 2.

The intensity factors (2) are such that the intensity becomes very small when the energy deviates appreciably from the straight lines of Fig. 1. The changes of frequency associated with an appreciable intensity are therefore smaller than predicted by Bitter, namely, of order  $\frac{1}{2} g\mu_0 H_0/\hbar$  instead of  $\frac{1}{2} g\mu_0 H_z/\hbar$ . Their detection will probably be rather difficult, as the mean position of the two components into which each Zeemann line is split weighted with their intensities, coincides with the position without radiofrequency field. The splitting would therefore have to be nearly resolved to detect significant changes in the polarization distribution on the Zeemann pattern.

<sup>1</sup> F. Bitter, Phys. Rev. 76, 833 (1949).

### The Beta-Spectrum of $\text{Ca}^{45}$ \*

P. MACKLIN, L. FELDMAN, L. LIDOFKY, AND C. S. WU  
Pupin Physics Laboratories, Columbia University,  
New York, New York  
November 21, 1949

**C**ALCIUM<sup>45</sup> was first produced in the cyclotron by bombarding calcium with deuterons or neutrons. The radioactivity consists of a soft beta-radiation of long half-life (152 days).

The upper energy of the  $\text{Ca}^{45}$  beta-spectrum is listed in Seaborg and Perlman<sup>1</sup> as 0.260 or 0.21 Mev by the aluminum absorption method and 0.25 Mev by spectrometer measurement. The details of the spectrometer measurement are unfortunately not available since they appear in the Plutonium Project Reports. The most recent value reported, 0.22 Mev,<sup>2</sup> was obtained by absorption methods.

Recently, we received a shipment of  $\text{Ca}^{45}$  from the Isotopes Division of the AEC at Oak Ridge of specific activity around 2  $\mu\text{c}/\text{mg}$  which is sufficiently high for investigation of the upper energy region of its beta-spectrum in our spectrometer. Several sources with approximate average thicknesses varying from 200-450  $\mu\text{g}/\text{cm}^2$  were prepared on collodion backings of 12-14  $\mu\text{g}/\text{cm}^2$ . The spectrum was investigated in the Columbia magnetic solenoidal spectrometer, using a counter with a collodion window of about 40  $\mu\text{g}/\text{cm}^2$  thickness and with three percent resolution (full

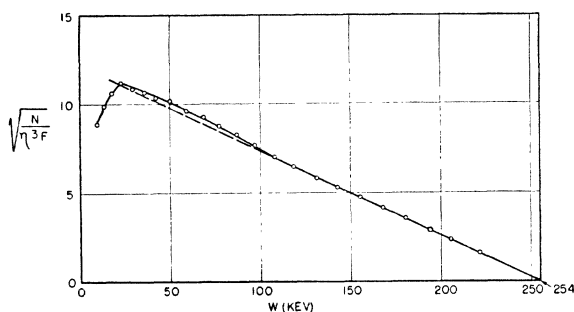


FIG. 1. Fermi plot of  $\text{Ca}^{45}$  beta-spectrum.

width at half-maximum). The end point of the spectrum as extrapolated from the Fermi plot is  $254 \pm 3$  kev. In constructing the Fermi plot, the non-relativistic Coulomb factor was used. A typical plot for a source of about  $200 \mu\text{g}/\text{cm}^2$  average thickness is shown in Fig. 1. The graph is linear from the end point to about 90 kev and deviates above the straight line below this energy. Previous experience in the investigation of low energy beta-spectra has shown that a  $200\text{-}\mu\text{g}/\text{cm}^2$  source has quite a distorting effect on the Fermi plot below 90 kev, yielding a greater relative abundance of slow electrons. We therefore attribute the non-linearity of the Fermi plot in the low energy region to the unfavorably thick source used and conclude that thinner and more uniform sources would probably yield a linear Fermi plot to energies below 90 kev.

The above end point combined with the half-life of 152 days gives an approximate  $ft$  value of  $0.7 \times 10^6$ , which empirically classifies  $\text{Ca}^{46}$  in the first-forbidden group. The linear Fermi plot is not contra-indicated by theory since, for certain types of interaction, a forbidden transition may yield a linear Fermi plot.

We should like to thank the U. S. AEC which aided materially in the performance of this research.

\* Partially supported by the AEC.

<sup>1</sup> G. T. Seaborg and I. Perlman, *Rev. Mod. Phys.* **20**, 592 (1948).

<sup>2</sup> J. L. Meem, Jr. and F. Maienschein, *Phys. Rev.* **76**, 328 (1949).

### Temperature Dependence of Scintillation Pulses in Anthracene\*

G. G. KELLEY AND M. GOODRICH

Oak Ridge National Laboratory, Oak Ridge, Tennessee

November 16, 1949

MEASUREMENT has been made of the decay constant and light output of anthracene scintillation pulses as a function of temperature. Values of the decay constant were obtained by photographing a series of individual pulses at each temperature using an oscilloscope with a vertical rise time of  $6 \times 10^{-9}$  sec. Because of statistical fluctuation in the individual pulses, many pulses had to be averaged in some manner. Two methods of averaging were used. First, exponentials were drawn by eye through twenty pulses selected at random at each temperature and averaged. Then on the suspicion of systematic errors, these twenty pulses were added graphically. This second method was employed at only two points because it was much more tedious and agreed with the first within two percent. It gave evidence, however, that the decay is exponential within the accuracy of the experiment over nearly a decade. Figure 1 shows the dependence on temperature. It appears to be linear with positive slope and to have an intercept with the temperature axis at  $-273^\circ\text{C}$ . The

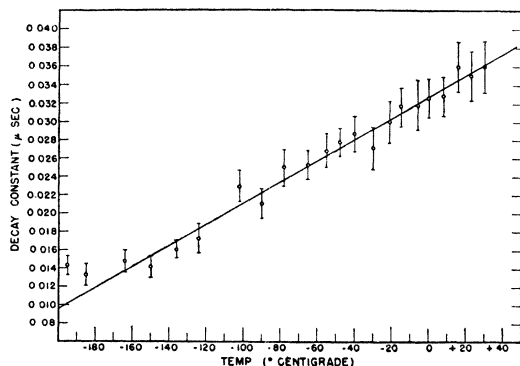


FIG. 1. Decay of scintillation pulses in anthracene. Brackets indicate 95 percent confidence interval based on spread of data.

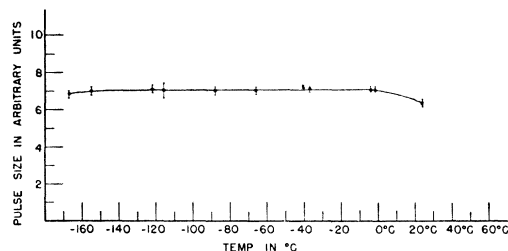


FIG. 2. Variation with temperature of the light pulse size in anthracene. (Conversion electrons from  $\text{Cs}^{137}$  measured with 1P28 photo-multiplier.)

decay constant at liquid nitrogen temperature is in agreement with the measurements of Collins.<sup>1</sup>

The temperature dependence of the size of the pulses has been investigated with a scintillation spectrometer of the type described by Jordan and Bell.<sup>2</sup> With a 1P28 photo-multiplier, the results, Fig. 2 show an essentially constant pulse size from room temperature to near liquid nitrogen temperature. With a 1P21 tube, however (results not shown), the pulses were some 30 percent larger at  $-60^\circ\text{C}$  than at room temperature. This confirms qualitatively earlier measurements made at this laboratory by P. R. Bell. Since the 1P28 tube has a lower short wave-length cut-off than the 1P21, it seems likely that the pulse size using the 1P21 may then be attributed either to a lowering of the short wave-length limit of its envelope or to a shift to higher wave-lengths of the scintillation spectrum. We have obtained spectrographic evidence for the former. Either explanation requires that the scintillation spectrum extend below 3400A which is the short wave-length cut-off of the 1P21. This is considerably lower than has been reported.<sup>3</sup>

\* This document is based on work performed under Contract No. W-7405, eng. 26, for the Atomic Energy Project at the Oak Ridge National Laboratory, Oak Ridge, Tennessee.

<sup>1</sup> George B. Collins, *Phys. Rev.* **74**, 1543 (1948).

<sup>2</sup> W. H. Jordan and P. R. Bell, *Nuclonics* **5**, 30 (1949).

<sup>3</sup> Louise Roth, *Phys. Rev.* **75**, 983 (1949).

### A $7 \times 10^{-9}$ sec. Isomeric State in $^{197}\text{Au}$ \*

F. K. MCGOWAN

Oak Ridge National Laboratory, Oak Ridge, Tennessee

November 10, 1949

USING sources of  $\text{Hg}^{197}$  and an experimental arrangement similar to that described in a previous letter,<sup>1</sup> an excited state of  $\text{Au}^{197}$  with a half-life  $(7.0 \pm 1.0) \times 10^{-9}$  sec. has been observed. In Fig. 1 the number of delayed coincidences is plotted as a function of delay time. The portion of the solid curve for delays less than  $3.5 \times 10^{-8}$  sec. and points indicated by circles represent the gross data. After subtraction of random coincidences the solid curve for delay time  $T \geq 3.5 \times 10^{-8}$  sec. represents the decay of the short-lived isomeric state which has been produced by the  $K$ -capture decay of  $\text{Hg}^{197}$ .

Figure 2 shows the number of coincidences as a function of delay time obtained with a source of  $\text{Te}^{126*}$  ( $\sim 58$  day). This resolution curve is typical of a negative result. The majority of the radioactive species investigated give similar curves exhibiting a sharp break at a delay of  $3.0$  to  $3.5 \times 10^{-8}$  sec. For larger delays the coincidence rate is constant and equal to the computed random coincidence rate.

The stilbene crystals, which are cemented to the tube envelope with Canada balsam, and Type 5819 multiplier tubes were operated at room temperature. The background (single counts) with phosphor in place is  $\sim 200$  c/m of which only 60 c/m is due to thermionic electrons leaving the photo-cathode. This corresponds to a pulse discrimination level such that incident radiation as low as 50 kev energy is detected.